Electronic Supplementary information (ESI)

Highly porous N-doped carbons impregnated with sodium for efficient CO_2 capture

Yun Kon Kim,[a] Gi Mihn Kim,[a] and Jae W. Lee[*a]

Department of Chemical and Biomolecular Engineering, Korea Advanced Institute of Science and Technology (KAIST), 291 Daehak-ro, Yuseong-gu, Daejeon 305-701, Republic of Korea

TABLE OF CONTENTS

A. Supplementary Results and Discussion

Thermogravimetric analysis

TGA analyses were carried out to confirm the thermal stability of Na_2CO_3, NS2, and SNS2-20 possessing Na_2CO_3 (Fig. S1). The weight decrease during the initial heating up stage up to 100 ℃ is attributed to the evaporation of surface water.[1] The weight of Na_2CO_3 keeps almost constant up to 900 ℃, and then, it gradually decreased with the increase of temperature because of the melting of Na_2CO_3.[2] For NS2, it lose its weight as much as 6 % up to heating temperature of 100 ℃, and the additional weight percent of 4 % was reduced until 630 ℃, which is related to the evaporation of interlayer water and the desorption of the adsorbed gas molecules. The steep decrease of the weight from around 700 ℃ is associated with the decomposition of the carbon support activated at 700 ℃. In the case of SNS2-20, it indicated large reduction (*ca.* 20 %) of the weight until 100 ℃, as it contained much water during the previous impregnation process. Then, the weight percent gradually decreased with the rise of heating temperature due to the decomposition of interlayer anions and, desorption of the adsorbed interlayer water and gas molecules.[3] In the range of 700 to 1000 ℃, the weight loss is due to the decomposition of carbon structure and strongly connected carbonate, considering the change of weight for Na_2CO_3 and NS2.[3]

Isosteric heats of adsorption[4, 5]

Isosteric heats of adsorption (Q_{st}) were estimated from the CO_2 adsorption isotherms data at 0, 25, 50 ^oC by means of the Clausius-Clapeyron equation.

The Clausius-Clapeyron equation for Q_{st} can be defined as,

$Q_{st} = RT^2 \left(\frac{\partial \ln p}{\partial T}\right)_q$ at constant adsorbate loading, q.

Where, R indicates the universal gas constant (kJ mol^{-1} K^{-1}); T temperature, P pressure.

The Ideal Adsorption Solution Theory (IAST) selectivity[6]

The IAST selectivity was calculated by fitting the pure component adsorption isotherms with a Single-site Lanngmuir equation for N_2 adsorption isotherms, and a Dual-site Langmuir-Freundlich equation for CO_2 adsorption isotherms, where the adjusted r^2 values for each fitted isotherm exceeded 0.999.

The equations can be defined as,

Single site Langmuir model[7, 8]

$$q = \frac{q_{sat} b p}{1 + bp}$$

Dual-site Langmuir-Freundlich model[9]

$$q = \frac{q_{sat,A} b_A P^{n_A}}{1 + b_A P^{n_A}} + \frac{q_{sat,B} b_B P^{n_B}}{1 + b_B P^{n_B}}$$

Where, q indicates the amount of CO_2 adsorbed (mmol g^{-1}); p is the pressure (bar); q_{sat} is the saturation loading (mmol g^{-1}); b is the Langmuir (bar) or Langmuir-Freundlich parameter (bar^{-n}) , and n is the dimensionless Langmuir-Freundlich exponent.

The IAST selectivity (S_{CO_2/N_2}) equation can be expressed using following equation

$$S_{CO_2/N_2} = \frac{\frac{q_1}{q_2}}{\frac{p_1}{p_2}}$$

Here, q_1 and q_2 denote the adsorption uptake of component 1 and 2, and p_1 and p_2 indicate the partial pressure of the 1 and 2. For the CO_2 : N_2 = 0.15 : 0.85 volume ratio, p_1 and p_2 represent 0.15 bar and 0.85 bar, respectively.

B. Supplementary Figures

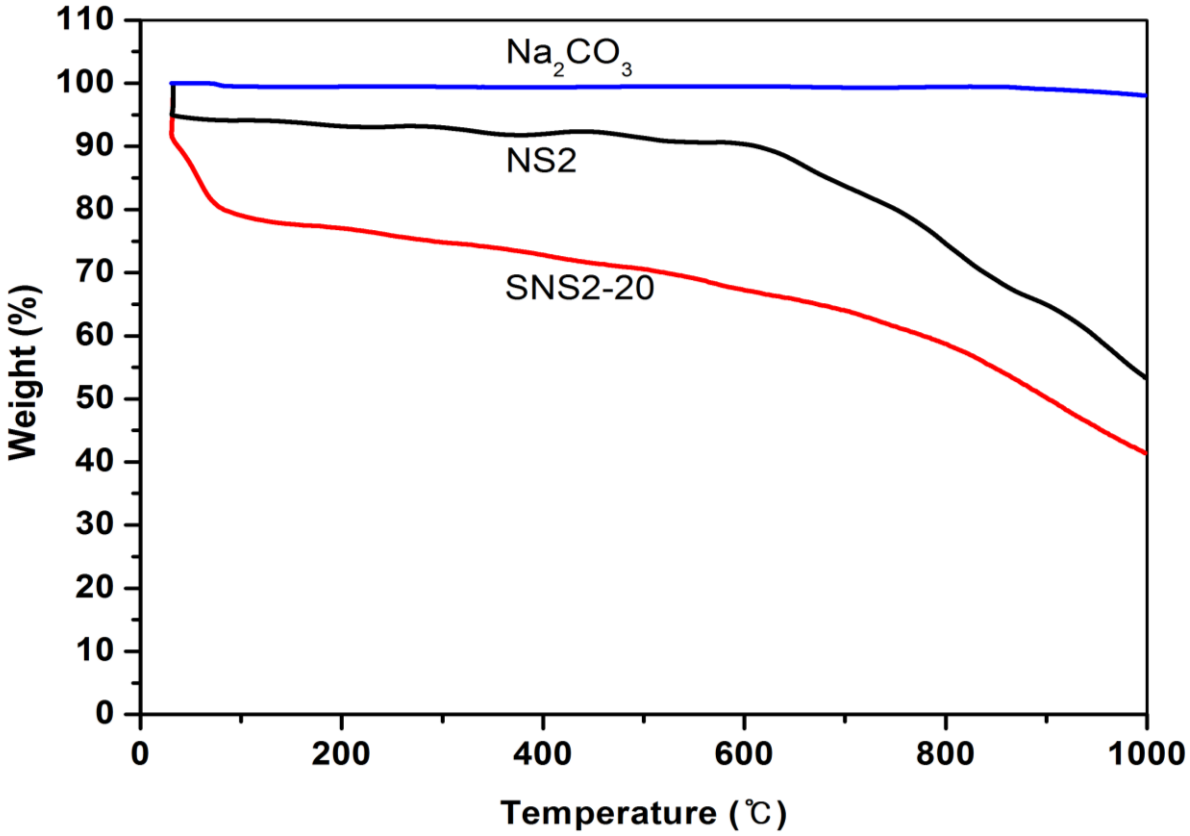

Fig. S1 TGA analyses of Na_2CO_3, NS2, and SNS2-20 under nitrogen atmosphere with heating rate of 10 ℃ min^{-1} up to 1000 ℃.

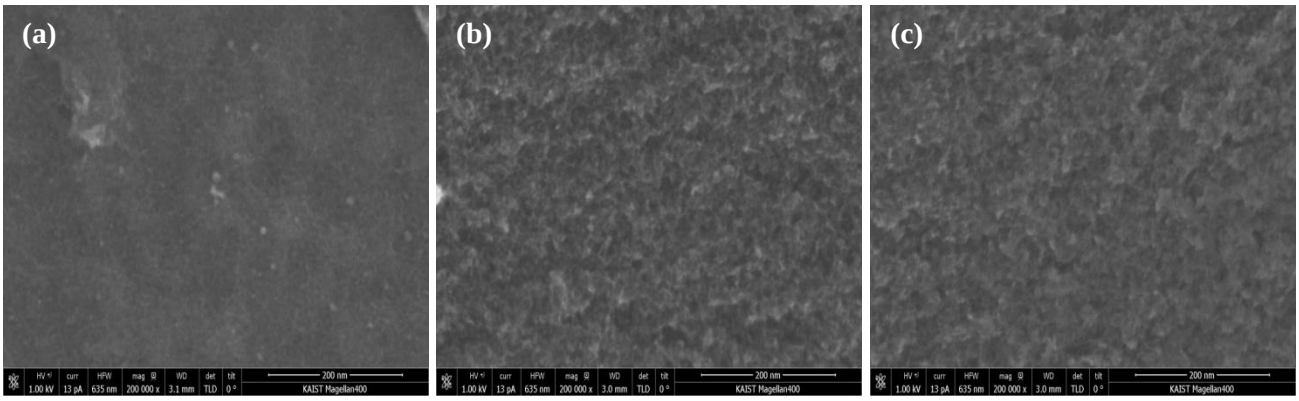

Fig. S2 SEM images of (a) NS1, (b) NS2, and (c) NS3.

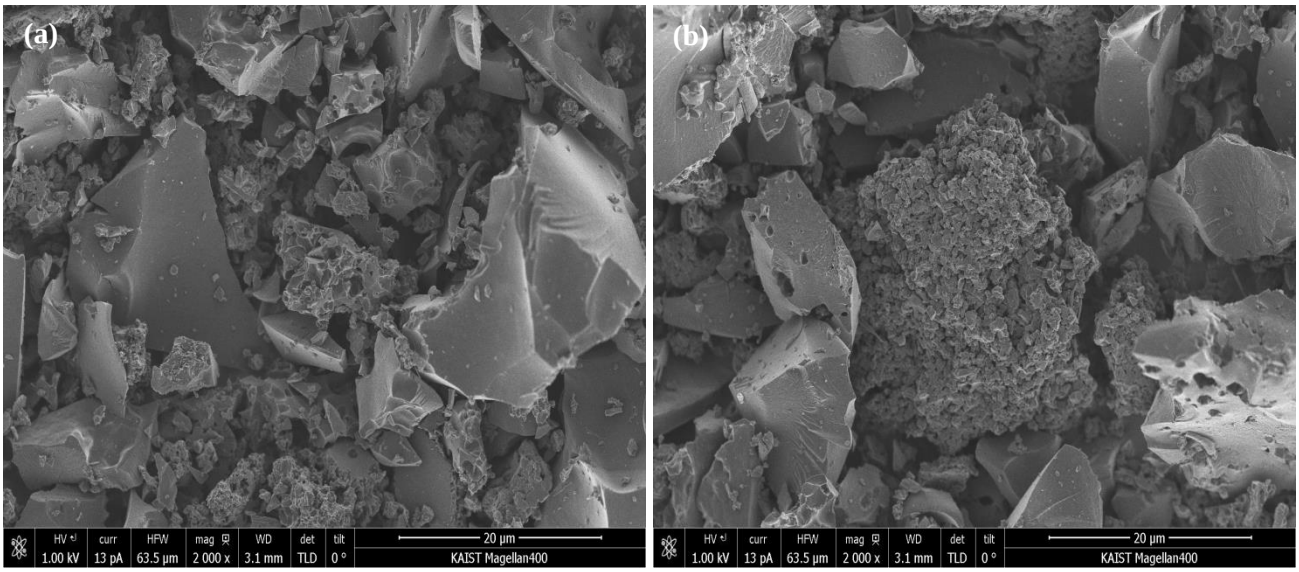

Fig. S3 SEM images of NaOH impregnated sample (a) SNS2-10 and (b) SNS2-20.

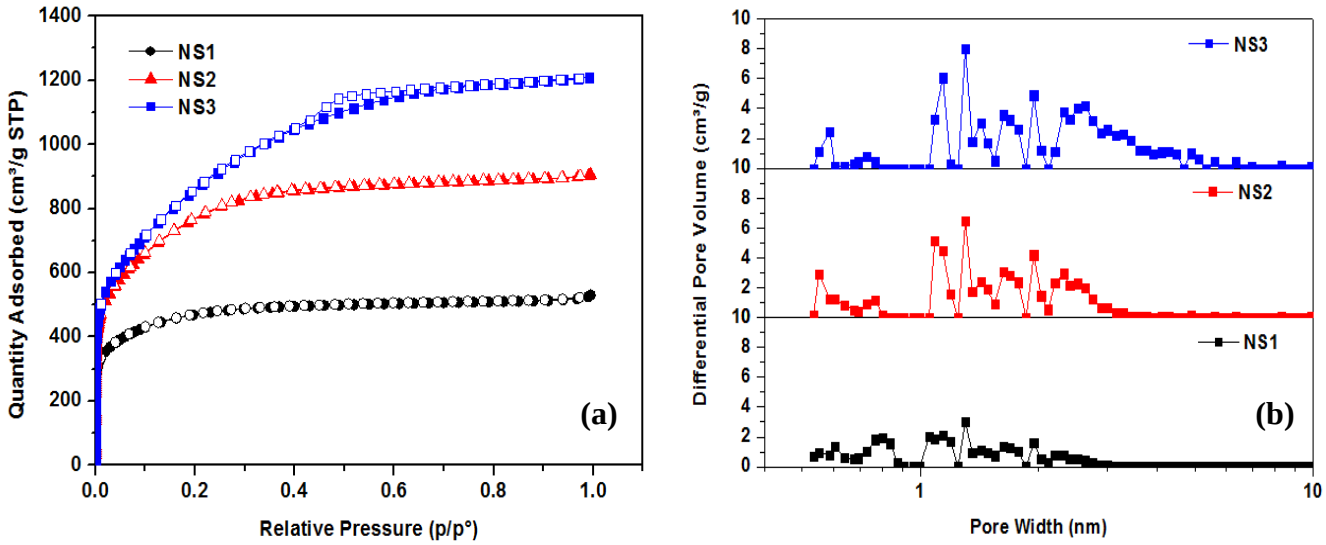

Fig. S4 (a) N_2 sorption isotherms at 77 K and (b) pore size distributions of NSs prepared with different KOH/PAN ratios.

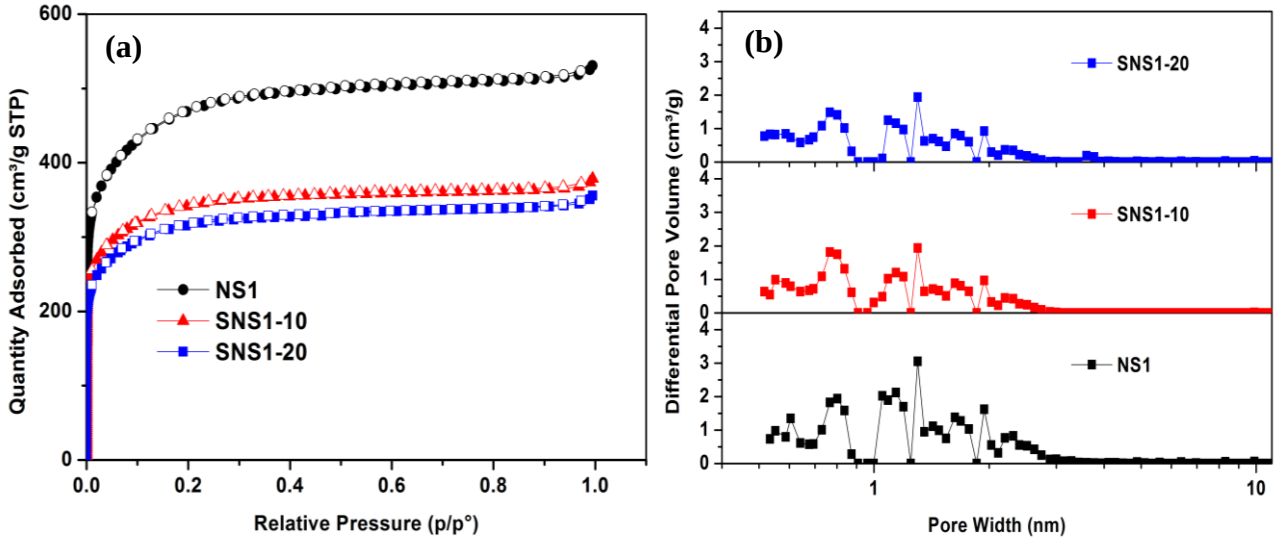

Fig. S5 (a) N_2 sorption isotherms at 77 K and (b) pore size distributions for NS1 and NaOH impregnated SNS1-10 and SNS1-20.

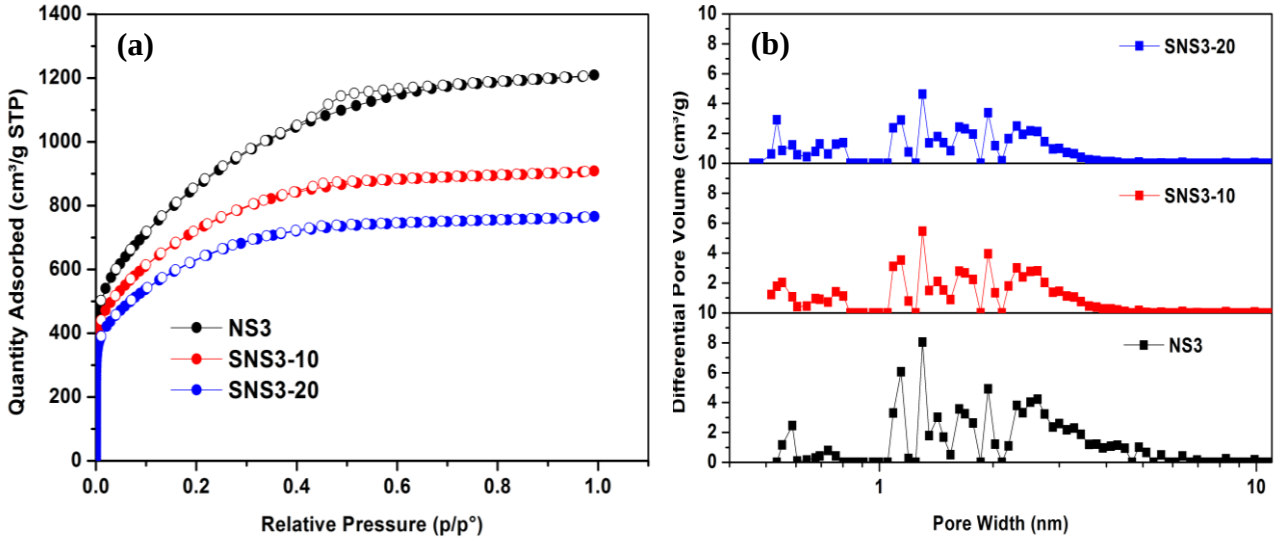

Fig. S6 (a) N_2 sorption isotherms at 77 K and (b) pore size distributions for NS3 and NaOH impregnated SNS3-10 and SNS3-20.

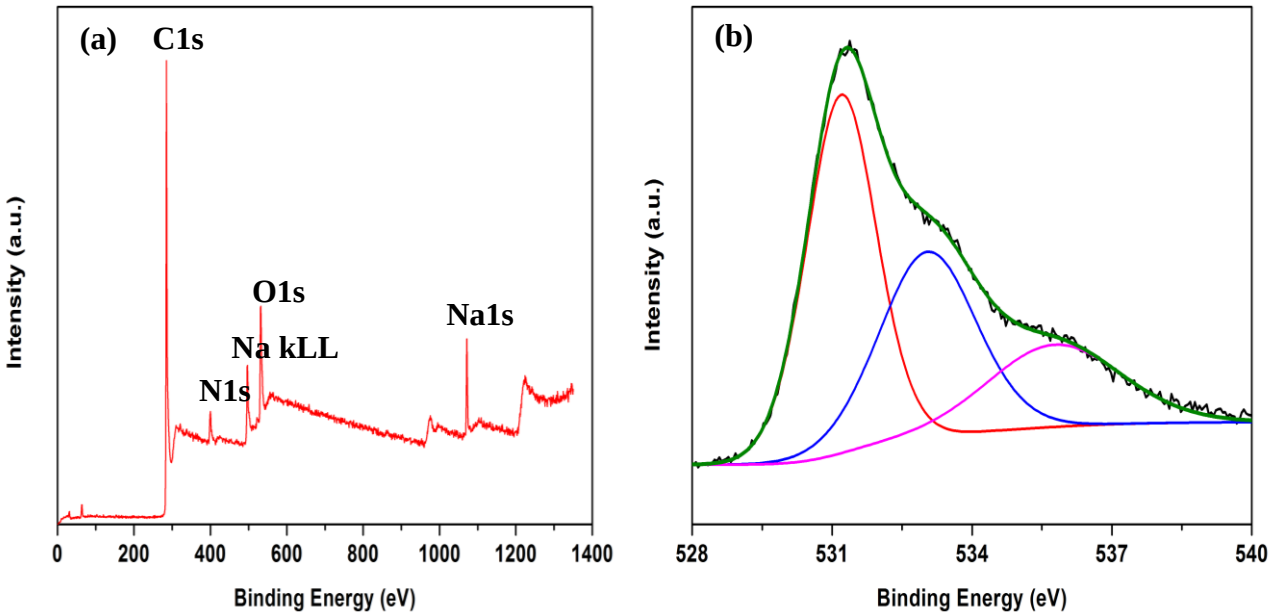

Fig. S7 XPS spectrum. (a) full survey spectra and (b) O 1s core level for SNS2-20.

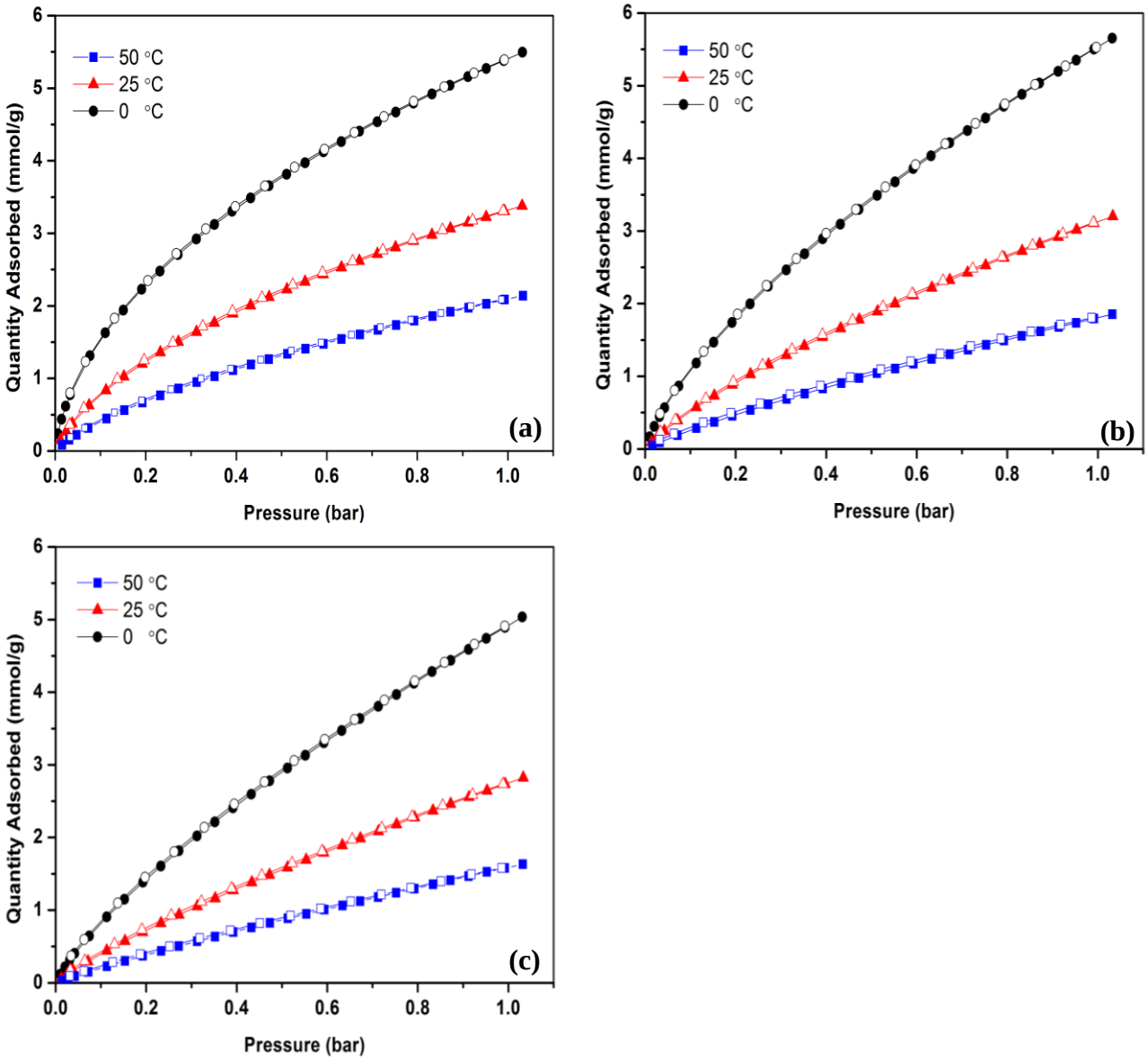

Fig. S8 CO_2 adsorption isotherms at 0, 25, and 50 °C (Closed markers: gas adsorption and open markers: gas desorption) for (a) NS1, (b) NS2, and (c) NS3.

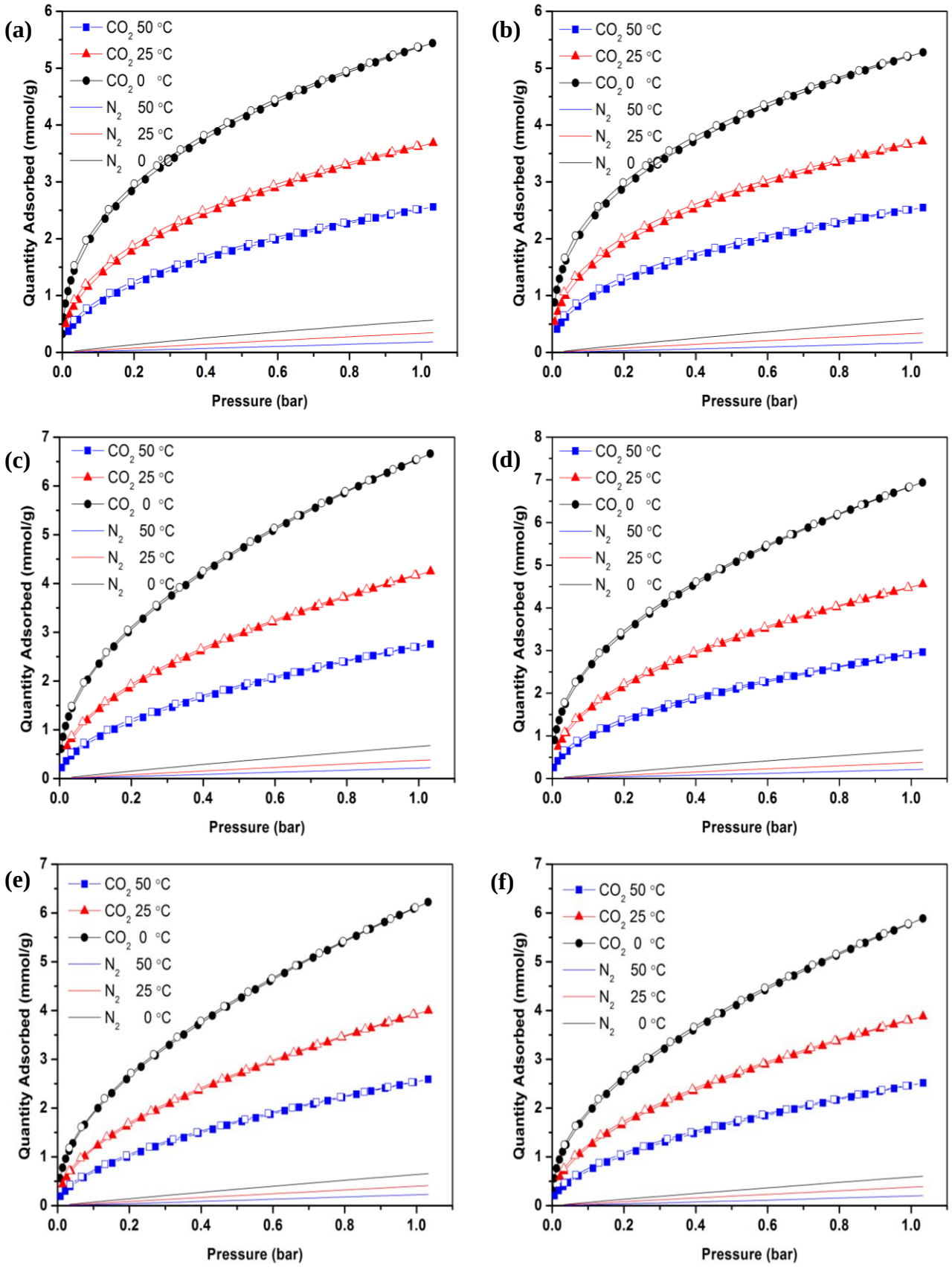

Fig. S9 CO_2 and N_2 adsorption isotherms (Closed markers: gas adsorption and open markers: gas desorption for (a) SNS1-10, (b) SNS1-20, (c) SNS2-10, (d) SNS2-20, (e) SNS3-10, and (f) SNS3-20.

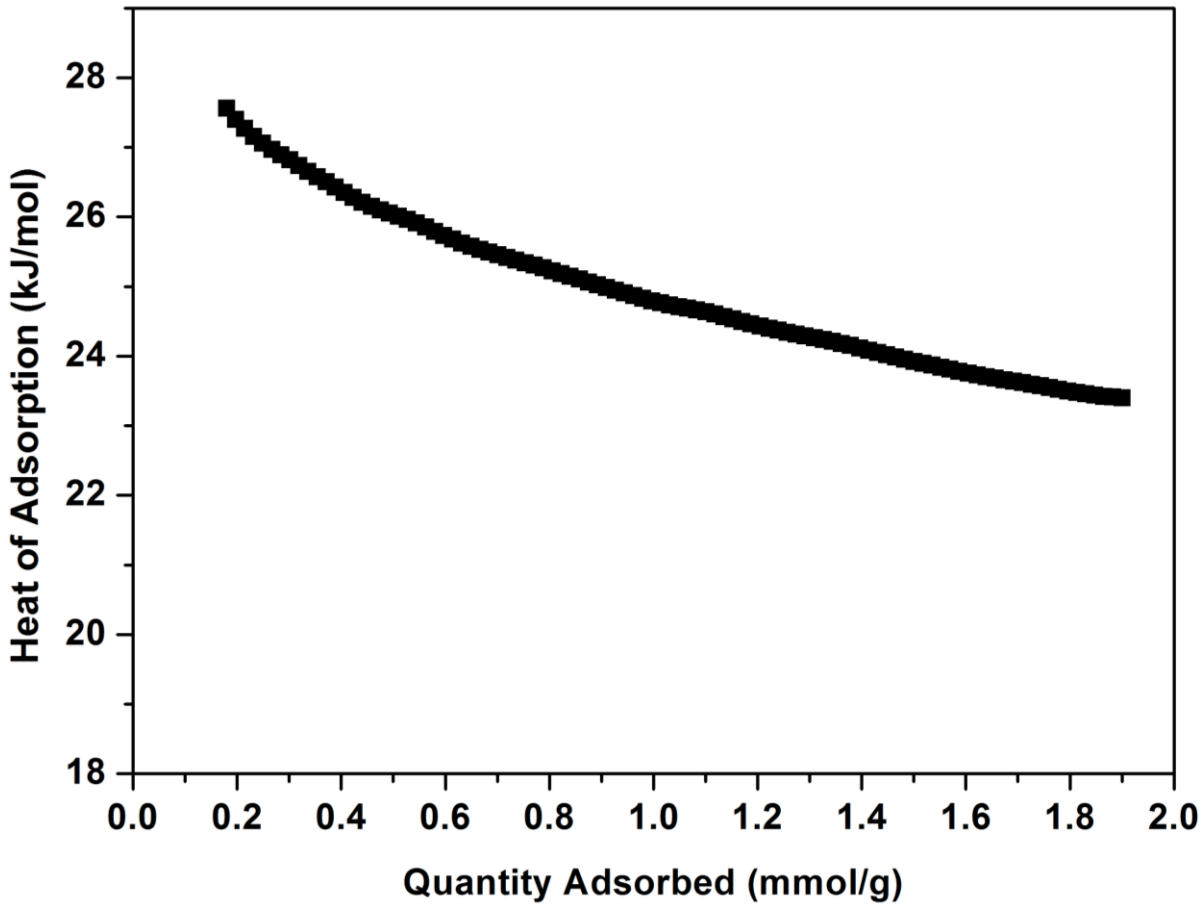

Fig. S10 Isosteric heats of CO_2 adsorption for NS2 estimated from the CO_2 adsorption isotherms at 0, 25, and 50 ºC.

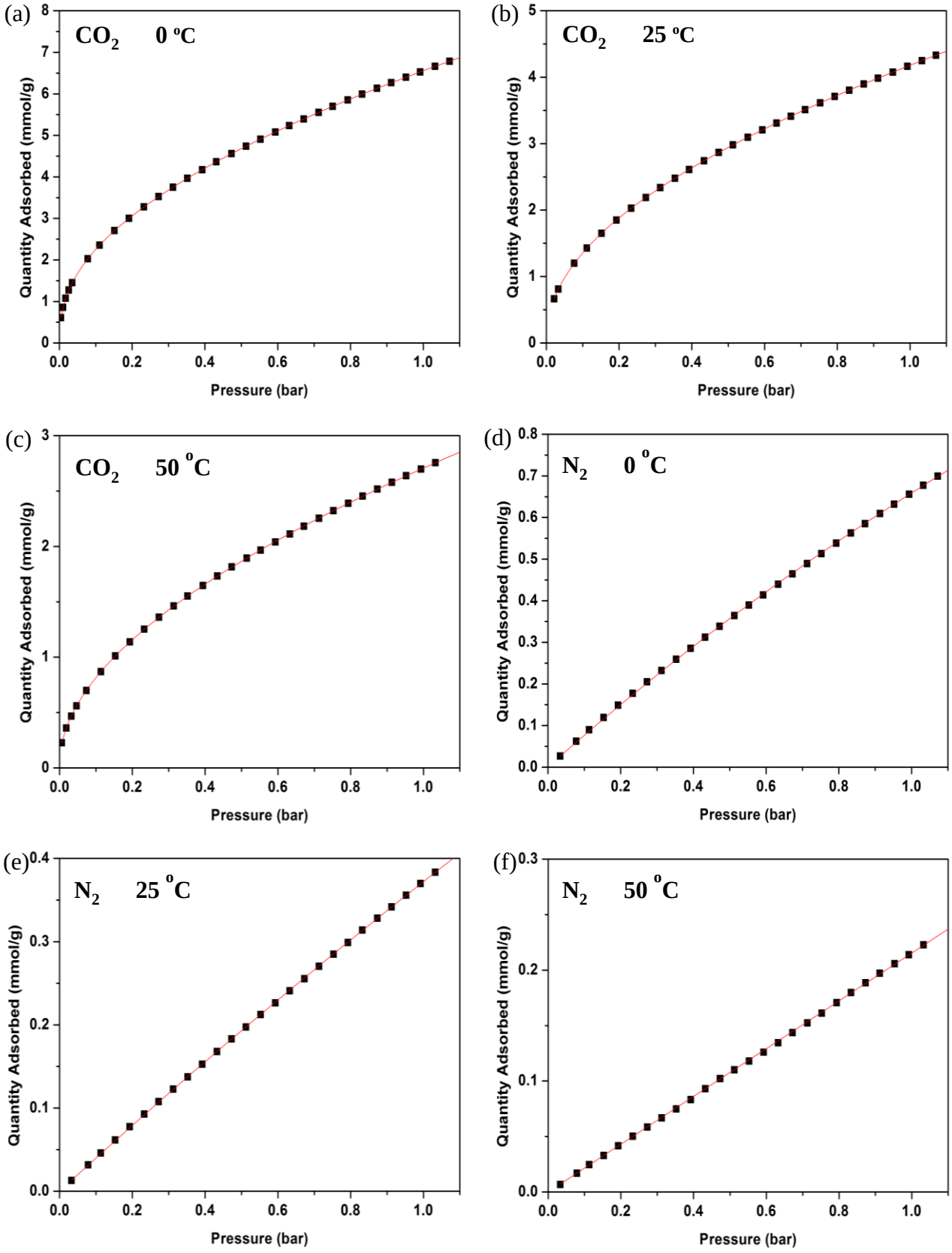

Fig. S11 Dual-site Langmuir-Freundlich equation fits for CO_2 adsorption isotherms of SNS2-10 at (a) 0, (b) 25, and (c) 50 °C. Langmuir equation fits for N_2 adsorption isotherms of SNS2-10 at (d) 0, (e) 25, and (f) 50 °C.

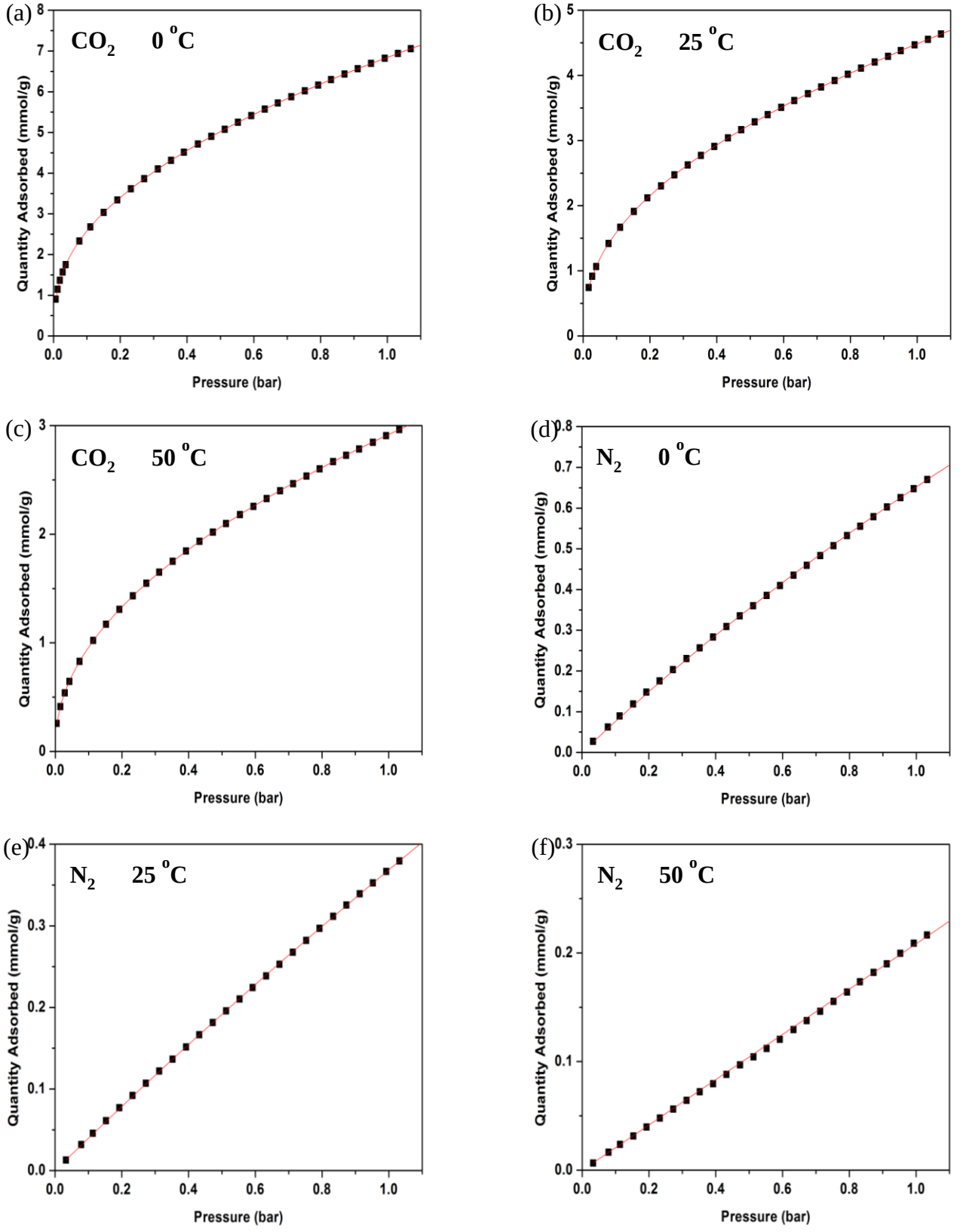

Fig. S12 Dual-site Langmuir-Freundlich equation fits for CO_2 adsorption isotherms of SNS2-20 at (a) 0, (b) 25, and (c) 50 °C. Langmuir equation fits for N_2 adsorption isotherms of SNS2-20 at (d) 0, (e) 25, and (f) 50 °C.

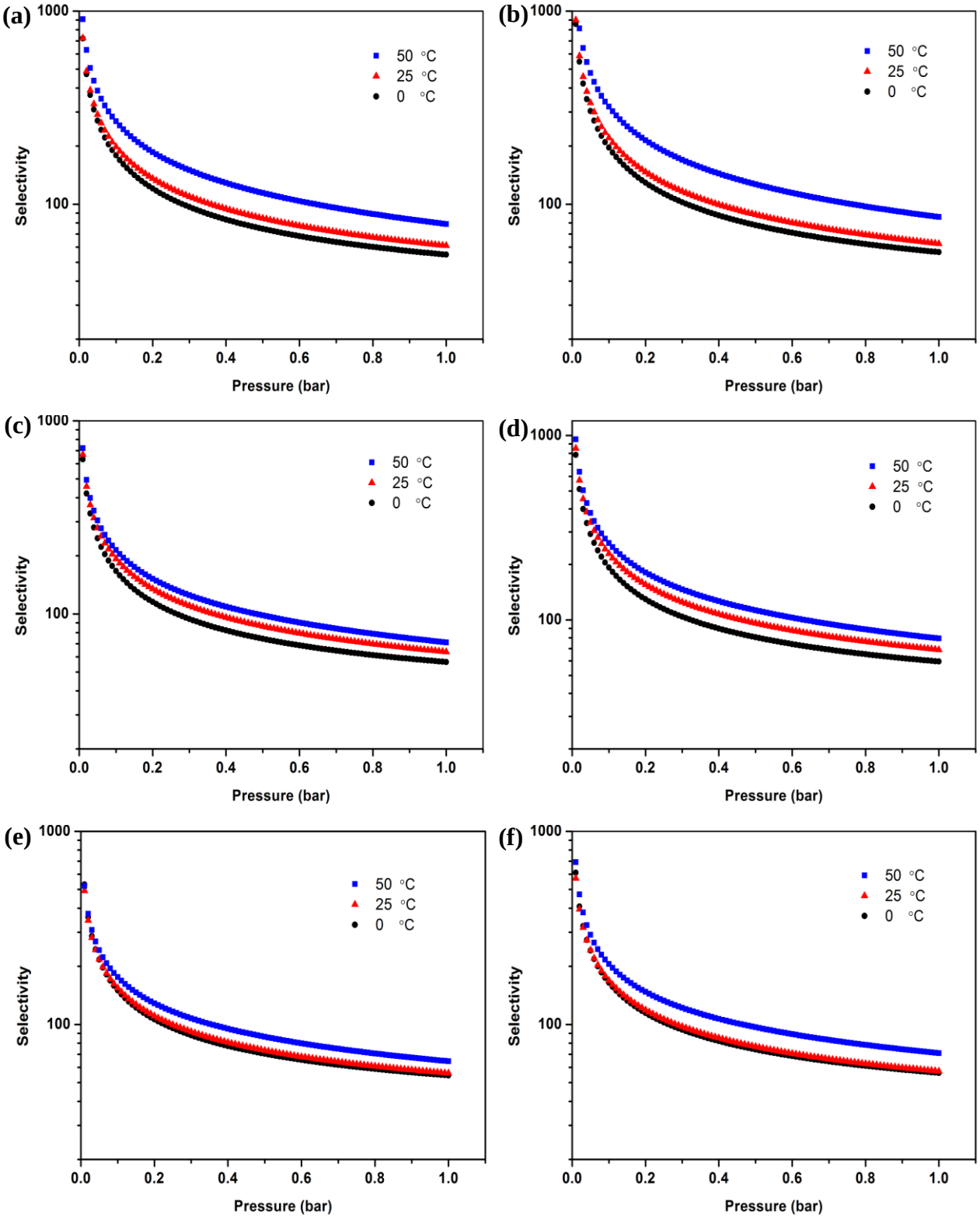

Fig. S13 IAST selectivies (CO_2 : N_2 = 0.15 : 0.85) at 0, 25, and 50 ºC for (a) SNS1-10, (b) SNS1-20, (c) SNS2-10, (d) SNS2-20, (e) SNS3-10, and (f) SNS3-20.

C. Supplementary Tables

Table S1 Chemical composition of NS1, NS2, NS3, and NaOH impregnated SNS2-10 and SNS2-20 by EDX analysis.

Elements	NS1		NS2		NS3		SNS2-10		SNS2-20	
	Weight%	Atomic%	Weight%	Atomic%	Weight%	Atomic%	Weight%	Atomic%	Weight%	Atomic%
N	6.49	5.66	4.73	4.11	2.77	2.40	3.58	3.34	3.83	3.51
C	89.99	91.64	92.26	93.59	94.72	95.70	71.05	77.12	79.90	85.46
O	3.52	2.69	3.01	2.29	2.51	1.91	20.80	16.95	7.92	6.36
Na	-	-	-	-	-	-	4.57	2.59	8.35	4.67

Table S2 Distributions of nitrogen configurations and total nitrogen amount measured by XPS.

Sample	Pyridonic / Pyrrolic (%)	Pyridinic (%)	Quaternary (%)	Pyridine Oxide (%)	$\pi - \pi^*$ (%)	Total N (atom %)
NS1	42.20	28.33	10.13	11.49	7.85	8.45
NS2	47.13	24.95	7.28	10.36	10.29	3.08
NS3	44.03	20.16	9.77	15.55	10.49	1.87

Table S3 Comparison of heat of ad(b)sorption for different sorbents

Sorbents	Heat of ad(b)sorption (kJ mol^{-1})[a)]	Reference
Ionic Liquids (ILs)	20	10
PPN-6-CH_2-DETA (PPNs)	56	5
UTSA-16 (MOFs)	53	11
1-en (MOFs)	49	9
Zeolite 13X	41	12
SA-2N-P (Carbon)	41	13
SNS2-20 (Carbon)	37	This work

a) Heat of adsorption of solid sorbents was estimated at 1mmol/g CO_2 loading.

Table S4 Dual-site Langmuir-Freundlich model parameters of the CO_2 adsorption isotherms for SNS2-10 at 0, 25, and 50 °C.

	0 °C	25 °C	50 °C
q_1 (mmol g^{-1})	25.11655	10.26224	5.03172
q_2 (mmol g^{-1})	13.23835	78.10675	90.26588
b_1 (bar^{-n1})	0.22506	0.331	0.17949
b_2 (bar^{-n2})	0.1719	0.02127	0.02199
n_1	0.40465	0.43595	0.34614
n_2	1.02378	0.8269	0.65334

Table S5 Single-site Langmuir model parameters of the N_2 adsorption isotherms for SNS2-10 at 0, 25, and 50 °C.

	0 °C	25 °C	50 °C
q (mmol g^{-1})	4.27706	5.06918	1681.32267
b (bar)	0.18214	0.0792	1.28×10^{-4}

Table S6 Dual-site Langmuir-Freundlich model parameters of the CO_2 adsorption isotherms for SNS2-20 at 0, 25, and 50 ºC.

	0 ºC	25 ºC	50 ºC
q_1 (mmol g^{-1})	6.94021	20.94423	5.32468
q_2 (mmol g^{-1})	17.45695	9.68185	189.91881
b_1 (bar^{-n1})	1.15028	0.0703	0.03728
b_2 (bar^{-n2})	0.21847	0.47307	0.01457
n_1	0.414	0.94866	0.12697
n_2	0.92021	0.43549	0.5284

Table S7 Single-site Langmuir model parameters of the N_2 adsorption isotherms for SNS2-20 at 0, 25, and 50 ºC.

	0 ºC	25 ºC	50 ºC
q (mmol g^{-1})	4.18027	4.85964	3046.3245
b (bar)	0.18469	0.08206	6.84×10^{-5}

D. Supplementary References

1. N. D. Hutson, S. A. Speakman and E. A. Payzant, *Chemistry of Materials*, 2004, 16, 4135-4143.
2. J.-W. Kim and H.-G. Lee, *Metall and Materi Trans B*, 2001, 32, 17-24.
3. Y. Min, S.-M. Hong, S. Kim, K. Lee and S. Jeon, *Korean J. Chem. Eng.*, 2014, 31, 1668-1673.
4. J. A. Mason, K. Sumida, Z. R. Herm, R. Krishna and J. R. Long, *Energy & Environmental Science*, 2011, 4, 3030-3040.
5. W. Lu, J. P. Sculley, D. Yuan, R. Krishna, Z. Wei and H.-C. Zhou, *Angewandte Chemie International Edition*, 2012, 51, 7480-7484.
6. A. L. Myers and J. M. Prausnitz, *AIChE Journal*, 1965, 11, 121-127.
7. J. Byun, S.-H. Je, H. A. Patel, A. Coskun and C. T. Yavuz, *Journal of Materials Chemistry A*, 2014, 2, 12507-12512.
8. H. A. Patel, S. Hyun Je, J. Park, D. P. Chen, Y. Jung, C. T. Yavuz and A. Coskun, *Nat Commun*, 2013, 4, 1357.
9. W. R. Lee, S. Y. Hwang, D. W. Ryu, K. S. Lim, S. S. Han, D. Moon, J. Choi and C. S. Hong, *Energy & Environmental Science*, 2014, 7, 744-751.
10. C. Wang, X. Luo, H. Luo, D.-e. Jiang, H. Li and S. Dai, *Angewandte Chemie International Edition*, 2011, 50, 4918-4922.
11. S. Xiang, Y. He, Z. Zhang, H. Wu, W. Zhou, R. Krishna and B. Chen, *Nat Commun*, 2012, 3, 954.
12. J.-S. Lee, J.-H. Kim, J.-T. Kim, J.-K. Suh, J.-M. Lee and C.-H. Lee, *Journal of Chemical & Engineering Data*, 2002, 47, 1237-1242.
13. X. Ma, Y. Li, M. Cao and C. Hu, *Journal of Materials Chemistry A*, 2014, 2, 4819-4826.